



## OPEN

SUBJECT AREAS:  
PRE-CLINICAL STUDIES  
BIOMEDICAL ENGINEERINGReceived  
7 August 2013Accepted  
12 December 2013Published  
10 January 2014Correspondence and  
requests for materials  
should be addressed to  
M.C.A. (christomark@  
gmail.com)

# Finite Element Modeling of A Novel Self-Expanding Endovascular Stent Method in Treatment of Aortic Aneurysms

Mark C. Arokiaraj<sup>1</sup> & Igor F. Palacios<sup>2</sup><sup>1</sup>Professor, Cardiology, Pondicherry Institute of Medical Sciences, Kalathumettupathai street, Kalapet, Pondicherry, India, <sup>2</sup>Cardiology Division, Massachusetts General Hospital, Boston, USA.

A novel large self-expanding endovascular stent was designed with strut thickness of  $70\ \mu\text{m} \times 70\ \mu\text{m}$  width. The method was developed and investigated to identify a novel simpler technique in aortic aneurysm therapy. Stage 1 analysis was performed after deploying it in a virtual aneurysm model of  $6\ \text{cm}$  wide  $\times$   $6\ \text{cm}$  long fusiform hyper-elastic anisotropic design. At cell width of  $9\ \text{mm}$ , there was no buckling or migration of the stent at  $180\ \text{Hg}$ . Radial force of the stents was estimated after parametric variations. In stage 2 analysis, a prototype  $300\ \mu\text{m} \times 150\ \mu\text{m}$  stent with a cell width of  $9\ \text{mm}$  was chosen, and it was evaluated similarly after embedding in the aortic wall, and also with a tissue overgrowth of  $1\ \text{mm}$  over the stent. The  $300/150\ \mu\text{m}$  stent reduced the peak wall stress by  $70\%$  in the aneurysm and  $50\%$  reduction in compliance after embedding. Stage 3 analysis was performed to study the efficacy of stents with struts (thickness/width)  $70/70$ ,  $180/100$  and  $300/150\ \mu\text{m}$  after embedding and tissue overgrowth. The adjacent wall stresses were very minimal in stents with  $180/100$  and  $70/70\ \mu\text{m}$  struts after embedding. There is potential for a novel stent method in aortic aneurysm therapy.

**A**ortic aneurysm is a common disorder, and it is due to weakening of the aortic wall due to weak collagen properties<sup>1</sup> or due to excess action of matrix metalloproteinase in certain patients<sup>2</sup>. Aneurysm rupture is a potentially life threatening complication<sup>3</sup>.

The treatment of aortic aneurysm would be by beta-blockers in initial stages, which reduce the aortic wall  $dP/dT$  (rate of change in the aortic wall pressure/rate of change of time) or rate of the rise of the aortic wall pressure<sup>3,4</sup>. Exclusion of aneurysm by Dacron or PTFE (Polytetrafluoroethylene) covered stent graft is a desirable treatment of choice at present in these patients. However, this has potential limitations such as side branch occlusion, endoleaks, paraplegia, device malfunctions and mal-appositions<sup>5-10</sup>. Endoleaks are seen in about  $29\%$  of the cases with endovascular repair<sup>8</sup>. There are difficulties in stent graft deployment and the procedure also requires adequate expertise and accuracy in deployment. Also, these stent grafts are bulky and have a large crimp profile. Femoral arteriotomy for vascular access by a surgeon would be frequently required in these patients before deployment. Flow exclusion by a multilayered nitinol model is another method of treatment of aneurysms and dissections of aorta<sup>11,12</sup>. We investigated a simple self-expanding Nitinol stent in the treatment of aortic aneurysms, and its effect on the aneurysm and aortic wall stress parameters. In this stent method, the flow was not excluded but instead the method preserves the existing aneurysm wall, and we analyzed the ability of the stent to absorb the stresses and strains in the aneurysm wall like a pillar.

## Results

**Buckling characteristics.** The buckling characteristics of the stent by cross sectional analysis after deployment in the aneurysm model is shown in figure 1. Stents with straight pattern buckle during deployment if cell size is  $< \sim 10\ \text{mm}$ , and with helical pattern buckle during deployment if cell size  $< \sim 8\ \text{mm}$ .

**Stress-strain, deployment and properties.** The principal and the peak-wall stresses, and the contact pressures before and after stent deployment of the  $70/70\ \mu\text{m}$  at  $0\ \text{mmHg}$ , and  $100\ \text{mmHg}$  are summarized in figure 2. At  $0\ \text{mmHg}$ , the principal stresses, and the peak wall stresses were negligible on the surface of the stent. The results of the  $70/70\ \mu\text{m}$  stent deployed in the aneurysm wall, and the effect of the stent on the maximal stresses and strain are summarized in figure 3. The stent could be deployed easily in the aneurysm model without redundancy. The stent apposes well on the aneurysm wall, and there was no buckling of the stent. There were only minimal stresses

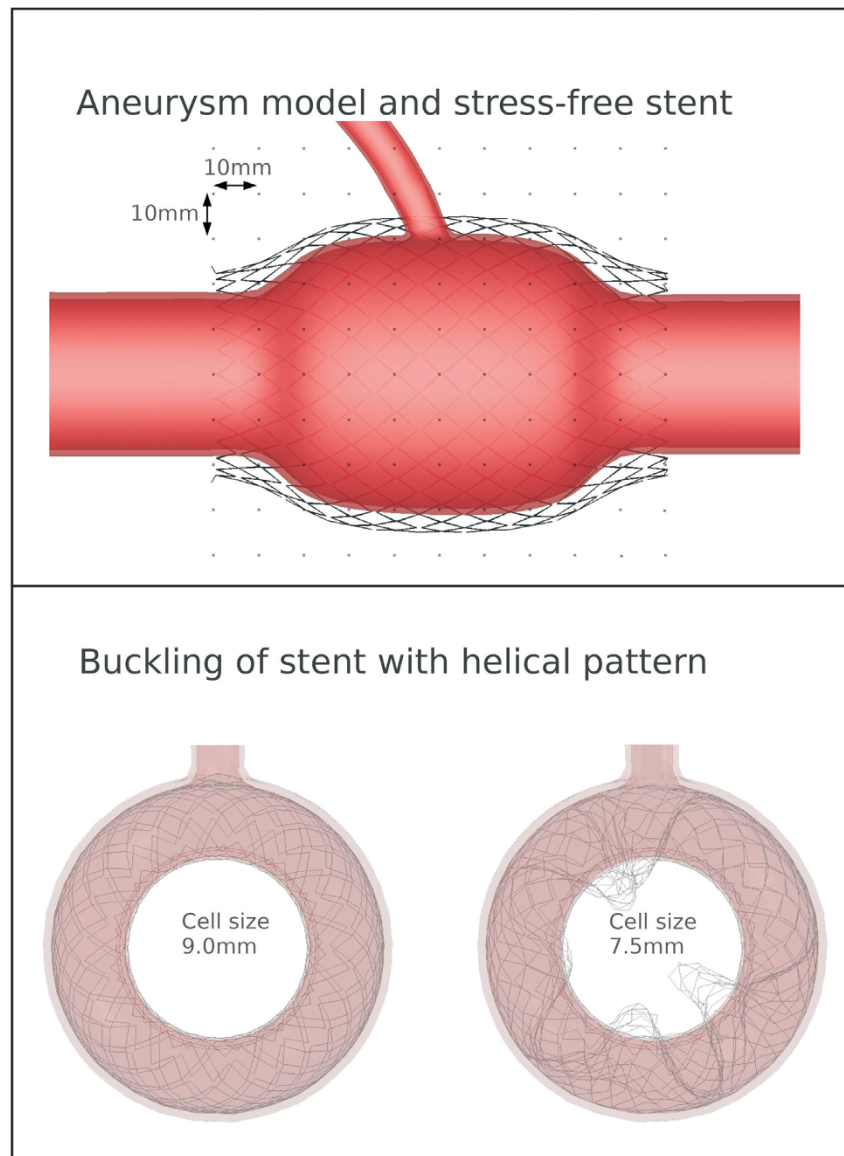


**Figure 1** | The upper panel shows an overlay of the stent over the aneurysm model. The stent is larger than the aneurysm and is deployed internally. The figure shows a cross sectional analysis of the stent deployed in 7.5 and 9 mm cell sizes. The cell width of 9 mm had no buckling as shown in the figure.

in the aneurysm and the adjacent aortic wall. There were no changes in strain parameters after stenting. There was good contact of the aortic wall and the stent. The observations demonstrated the efficacy of the stent, and its benign stress characteristics on the aneurysm wall after deployment. There was no change in aneurysm size after 70/70  $\mu\text{m}$  stent deployment, which was an important observation to demonstrate the efficacy of the stent in stage 1 analysis.

**Migration and crimp characteristics.** There was no migration of the stent when studied at a blood pressure (BP) of 180 mmHg. This stent could be crimped in a 9 F catheter. This is due to lesser metal load and larger cell widths and absence of Dacron cover when compared to conventional endovascular stents. This advantage would be very useful to the interventionist as the procedure could be easily performed through percutaneous route even by basic interventionists.

**Radial force evaluation.** Results of the radial force evaluation (figure 4) of the stent showed a minimal radial force on the aortic wall of the 70/70 and 180/100  $\mu\text{m}$ . The radial force was highest in 300/150  $\mu\text{m}$  stent, when compared to stents with other strut dimensions. The radial force was markedly low in the 70/70  $\mu\text{m}$

stent. Cell widths did not affect the radial forces for the 70/70  $\mu\text{m}$  and 180/100  $\mu\text{m}$  stents. However, in the 300/150  $\mu\text{m}$  stent, higher cell widths (7.9 and 9.5 mm) were associated with higher radial strength. Hence, the 300/150  $\mu\text{m}$  stent had desirable stress characteristics and adequate radial force at 9 mm cell widths. The commercially available self-expanding stents have a radial force of 2 to 5 N.

**Stage 2 results of 300/150  $\mu\text{m}$  stent after embedding.** Stage 2 study results with 300/150  $\mu\text{m}$  stent model after embedding in the aortic wall with tissue overgrowth are shown in figure 5. In the panels 3 and 4, the peak wall stresses were remarkably lesser after embedding the stent than in other panels before and after stent deployment. The stent reduced the peak wall stress by 70% in the aneurysm after a tissue overgrowth of 1 mm over the stent struts (Figure 5). Also, there was a 1.2 mm increase in the aneurysm size after deployment of the stent. This is a very mild increase in aneurysm size, which is not desirable. However, this occurs at a significant fall in wall stresses, which is very advantageous. This negligible increase in aneurysm diameter (1.2 mm at 0 mmHg, 0.6 mm at 100 mmHg and 0.1 mm at 180 mmHg) is not seen in other endovascular treatment methods. The stent primarily absorbs stresses and it also preserves the native function of the vessel.

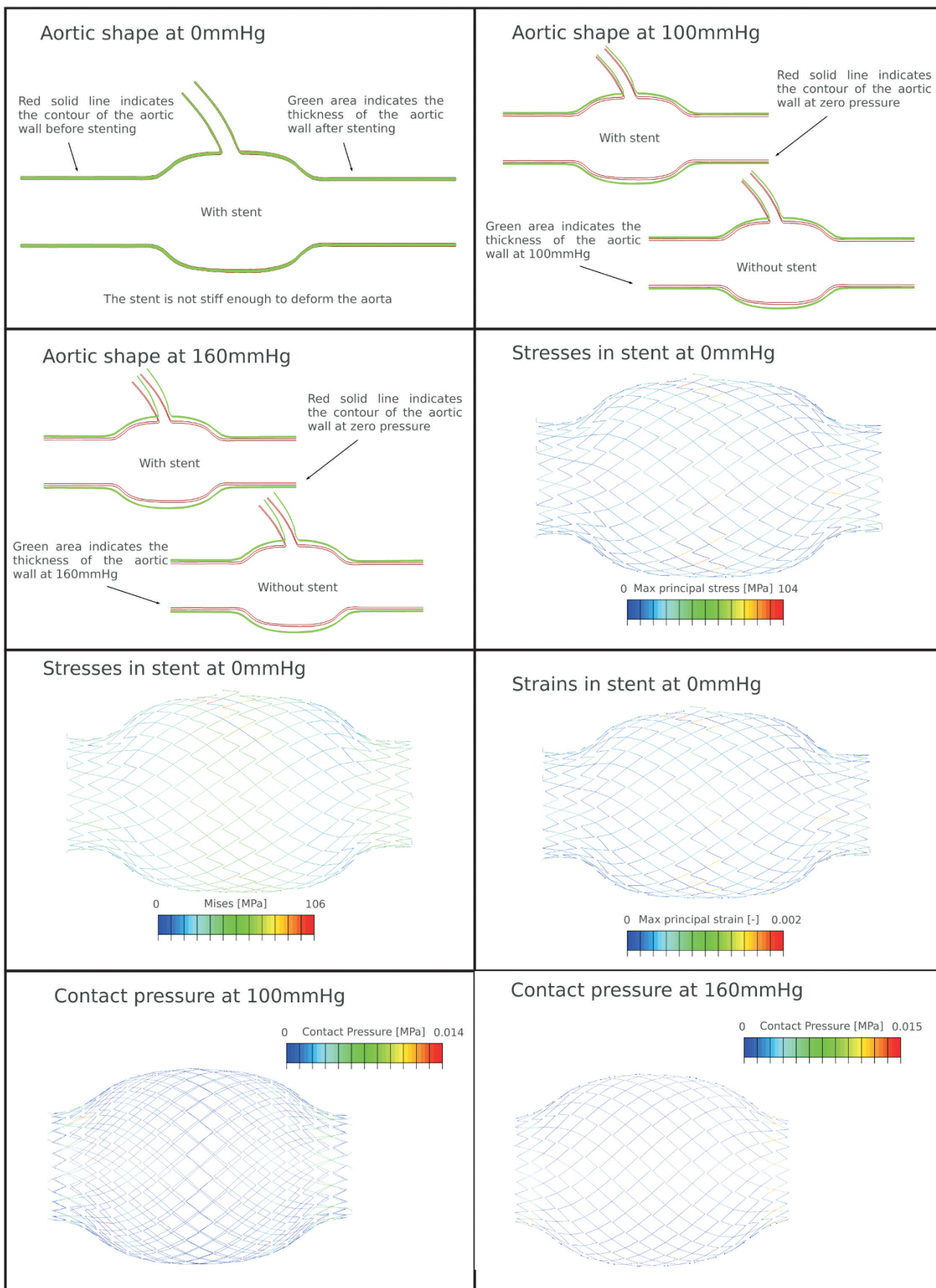


**Figure 2** | The upper panels show the aortic shape before and after stenting at 100 and 160 mmHg pressures. Stress and strain distribution, and the contact pressures in the aortic wall after deployment of 70/70  $\mu$ m at 0 mmHg and 100 mmHg.

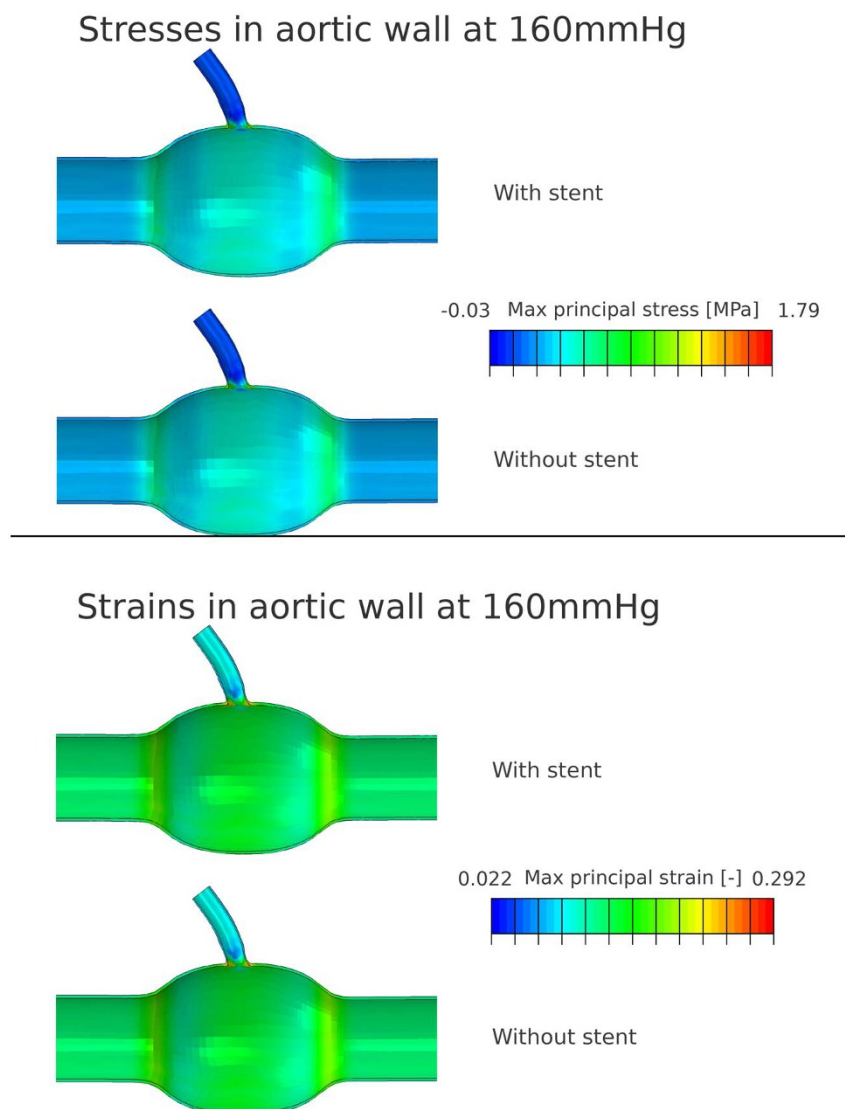


**Figure 3** | Stress distribution and strain of the aorta before and after stenting with the 70/70  $\mu\text{m}$  Nitinol stent at 160 mmHg.

The aneurysm wall compliance reduced by 50% after stent deployment. The aortic diameter variation (Table 1) during a cardiac cycle (Blood pressure from 100 to 180 mmHg) reduced from 2.6 mm without stent to 1.4 mm with embedded stent, and 1.2 mm with embedded stent and significant tissue overgrowth.

**Stage 3 study results of stents with various strut dimensions after embedding.** Stage 3 study results have shown a significant reduction in the aortic wall stresses by all the 3 stents with various strut thicknesses. Stress values and distribution in the aneurysm are similar in the investigated cases. However, smaller struts reduce the higher stress value at the aneurysm ends (figure 6). Table 2 summarizes the results of aortic diameter variation with stents of various strut dimensions. At zero pressure larger struts correspond to higher aortic diameter (AD). When the pressure rises larger struts are stiffer and tend to reduce the AD increment. Larger struts reduced AD variation efficiently during a cardiac cycle.

## Discussion

This is a proof of concept analysis, which demonstrates the theoretical potentials of the novel Nitinol based self-expanding stent in the treatment of aortic aneurysm. The stent had a good radial strength, and it reduces maximal stress distribution in aneurysm wall by more than 70%. The stent is novel as it is very large in diameter (70 mm)

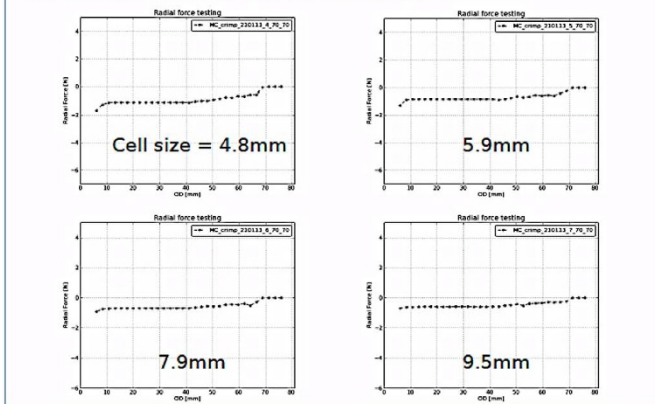
with a low crimp profile, and large (9 mm) cell width with an adequate radial force (1 to 5 N), and it also hugs the entire wall of the aneurysm sac in all dimensions, which is conceptually unique. The currently available largest diameter of an uncovered or bare peripheral arterial stent is only 14 mm. Commercially available uncovered venous stents have a maximum diameter of 28 mm (Sinus stent, Optimed). Balloon expandable uncovered Palmaz-Genesis (Cordis) peripheral stent has a maximal dimension of 22 mm, which is expandable to about 26 mm.

This method is conceptually very different from the endovascular stent grafts, which is bulky, expensive and technically demanding, and it is associated with various complications<sup>7–10</sup>. Also, this is distinctly different from the multilayered flow diverting stent which functions by inducing thrombosis in the multilayered stent to exclude the flow to the aneurysm wall to a significant extent<sup>11,12</sup>. This method could also be initiated as an initial method of therapy, which could be adequately revised with endovascular stent grafts or flow diverting stents in later stages of disease progression, if required.

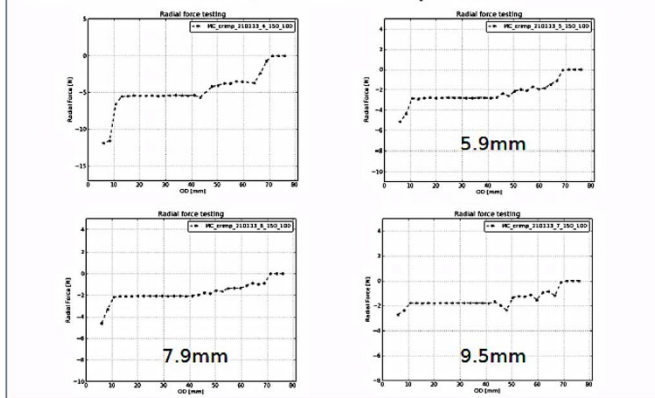
The study stent's width is 70 mm in maximum diameter. The stent has a low crimp profile of 9 F compared to that of stent grafts (18–21 F minimum) for a caliber of  $> 40$  mm stent-graft. Hence, surgical arteriotomy would not be required in our method, and also the puncture site complications, which could be at times be life threatening, would be minimal.



### Radial force testing – results strut thickness/width: 70/70



### Radial force testing – results strut thickness/width: 180/100



### Radial force testing – results strut thickness/width: 300/150

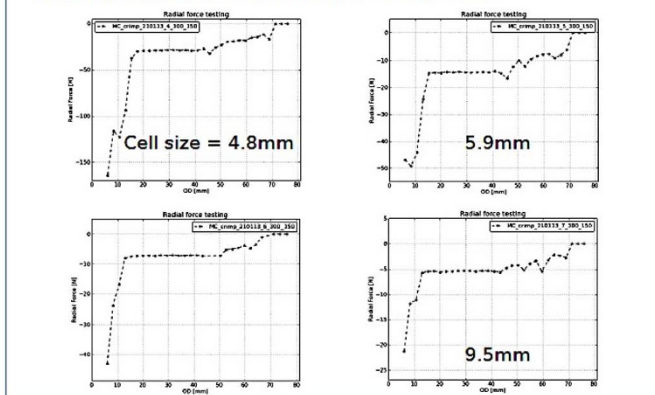


**Figure 4** | Results of the radial force testing of the stents at various (70/70, 180/100 and 300/150  $\mu\text{m}$ ) strut dimensions.

Before stenting, the stress inside the aneurysm wall was two times higher than in the healthy aortic wall (0.30 vs. 0.15 MPa at BP = 100 mmHg). After stenting and stent embedding, the stress on the aneurysm wall was reduced by  $\sim 70\%$  (from 0.30 to 0.10 MPa at Blood pressure of 100 mmHg, from 0.40 to 0.15 MPa at BP = 180 mmHg), and it was lower than the stress in the healthy aorta (0.15 MPa at BP = 100 mmHg and 0.25 MPa at Blood Pressure = 180 mmHg). The higher beneficial effect at 180 mmHg could be due to reduction in compliance, and a higher elastance and windkessel

effect at that pressure (180 mmHg). When the wall stress reduces the risk of aneurysm rupture would be less as shown in computational and in-vivo studies<sup>13–17</sup>.

The stent could be easily deployed in the aneurysm model, and the crimp profile was moderate (9 F). This low crimp profile is comfortable for any basic operator to use. The stent mildly increased the aortic aneurysm diameter size by about 1.2 mm (Table 1). A stent embedded in the aneurysm wall decreased the aneurysm wall compliance by more than 50%, and there was a marked decrease in the aneurysm diameter change at 100 mmHg and 180 mmHg, which is a reduction from 2.6 mm to 1.2 mm. The impact of the 9 mm cell size stent on aortic shape, stresses, and strains are negligible with respect to the impact of blood pressure. The stent did not increase the stresses and strains in the aortic aneurysm wall after deployment (Figure 3). This was essential to prove the concept that the method does not harm the existing aneurysm and the adjacent aorta, as the primary concept appears counter-intuitive.

Stent migration did not occur when modeling at a blood pressure of 180 mmHg, which is another important observation in the study. This could be due to self-expanding nature and good apposition of the stent onto the aortic wall, and also due to fixation of the stent by the barbs.

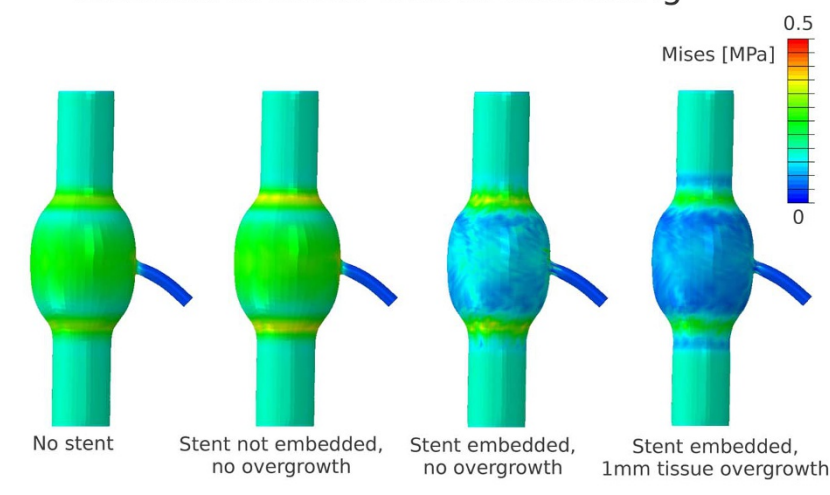
The impact on the daughter artery by the stent was negligible by pressure analysis. The daughter artery had a diameter of 7 mm and the cell width of the stent was 9 mm, which is adequate to maintain blood flow easily in the daughter artery. The current commercially available peripheral stents<sup>18,19</sup> have a cell width of about 2 mm. Hence, after deployment of a conventional stent in this model about 12 meshes would be across the origin of the daughter artery, whereas only one cell crosses the origin with the described design of 9 mm cell width. Hence, this stent has a very high probability of preservation of flow in the daughter artery. Though clot formation is mediated by platelets, the trigger by metal load, due to the crossing struts would be significantly lower in the current stent method due to wider cell widths. When compared to endovascular repair where the daughter artery is entirely excluded, this stent due to wider cell widths could easily preserve the side branches. Compared to the flow diverting stents the theoretical probability of side branch occlusion would be minimal as this method is single layered. The stresses at the origin of the daughter artery were reduced after deployment of the stent when compared to baseline (Figure 5, panels 3 and 4).

At the edges of the stent, there were no abnormal stresses on the normal aorta as this is very essential to prove that the stent does not harm the normal adjacent aorta. The effect was more pronounced in stents with thinner (70/70 and 180/100  $\mu\text{m}$ ) struts, than stents with thicker struts (300/150  $\mu\text{m}$ , figure 6). The effect of the stent on the aneurysm's wall stresses needs to be studied further over a period of time.

The stent had maximal reduction in the wall stresses when it is embedded and with a tissue overgrowth. The method does not have any benefit without embedding the stent in the aortic wall. In real life situation, there will not be an adequate tissue cover over the entire stent. Hence, the results in real life situation would be in-between panels 3 and 4 in Figure 5. The success of this method depends on embedding the stent and promoting tissue overgrowth, which is a part of vascular remodeling after stent deployment<sup>20–23</sup>. To enhance tissue overgrowth the stent could be coated with a polymer base as a carrier with vascular endothelial or fibroblastic growth factors. Though speculative, biological materials or hydrogels may be used for better adhesion of the stent, and possibly this would enhance tissue proliferation. For instance, certain hydrogels are useful to enhance tissue engineering and growth of scaffolds<sup>24</sup>, and studies have demonstrated manipulations in overlying endothelial cells can have changes in the underlying extra-cellular matrix and smooth muscle cells<sup>23,25</sup>. In economic perspectives, smearing of alcohol in appropriate concentrations or perhaps pluronics on the stent could



## Stresses in aortic wall at 100mmHg



## Stresses in aortic wall at 180mmHg

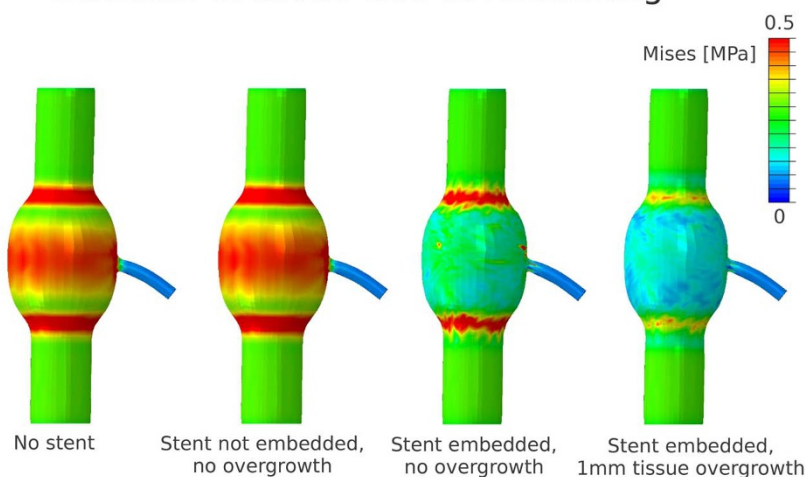


**Figure 5 |** The maximal stress distribution pattern in the aortic wall after deployment of 300/150  $\mu\text{m}$  in the wall at 100 mmHg and 180 mmHg is depicted. There are 4 panels. The first panel has no stent, the second panel has stent deployed, the third panel has the stent embedded, and the fourth panel shows the stent embedded with tissue growth.

be used to study tissue proliferation. The effect of overlapping two stents with a different design in the same model needs to be evaluated further.

In the past, wall stent has been modeled mathematically as a bare stent, and it was compared with endovascular graft prosthesis in the treatment of aneurysms<sup>26</sup>. In this mathematical analysis<sup>26</sup>, the wall stent had a maximum diameter of 24 mm only, and it was used as a skeleton of endovascular prosthesis and analysis was performed compared to stent graft. Hence, the concept in the mathematical modeling was very different from our stent method developed in this study by finite element analysis.

Multiple wall stents have been used in the therapy of aneurysm<sup>27,28</sup>. Conceptually in this study from China, where flow diversion stents

were not available, the wall stents were deployed serially. They were used to form like a flow modular or diversion stent, and they cover the entire segment i.e. normal-normal segment across the aneurysm, and the stents diameter ranged from 20 to 28 mm only. Tang Xiao et al reported a significant negative result with that technique<sup>28</sup>.

Computational and in-vivo studies in the past have proved that reduction of wall stresses result in a significant reduction in the rate of growth of aneurysm<sup>29–32</sup>. This study stent technique is distinctly different from multilayered stent, which excludes the flow and does not appose on the aneurysm wall.

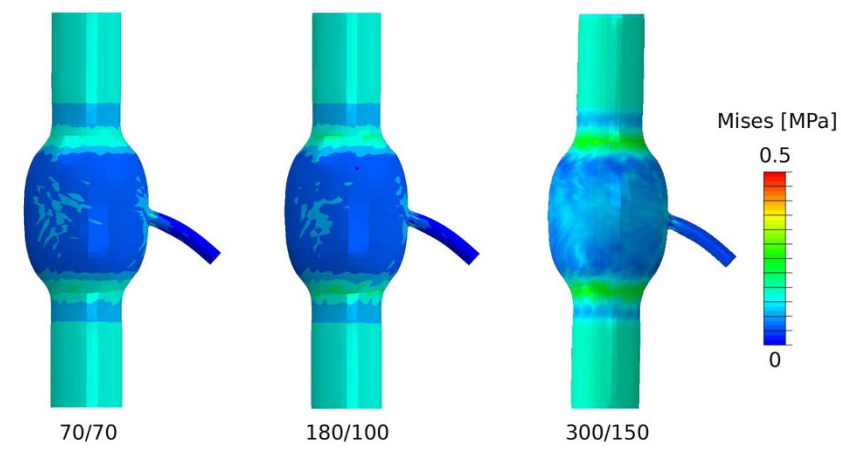
This self-expanding stent method by reducing the wall stress would prevent aneurysm expansion. However, this may not help in aneurysm shrinkage, which would be ideal. This method could be

**Table 1 |** The aneurysm diameter (AD) is shown with or without stent deployment and the results after embedding the stent into the aortic wall and thereafter, with a tissue overgrowth of 1 mm over the 300/150  $\mu\text{m}$  stent

Maximum aneurysm diameter, (mm)	No stent	Stent not embedded, no overgrowth	Stent embedded, no overgrowth	Stent embedded, 1 mm tissue overgrowth
AD <sub>0</sub> (0 mmHg)	59.4	60.7	60.7	60.7
AD <sub>100</sub> (100 mmHg)	65.8	66.1	64.1	63.2
AD <sub>180</sub> (180 mmHg)	68.4	68.5	65.5	64.4
AD <sub>180</sub> –AD <sub>100</sub>	2.6	2.4	1.4	1.2



## Stresses in aortic wall at 100mmHg



## Stresses in aortic wall at 180mmHg

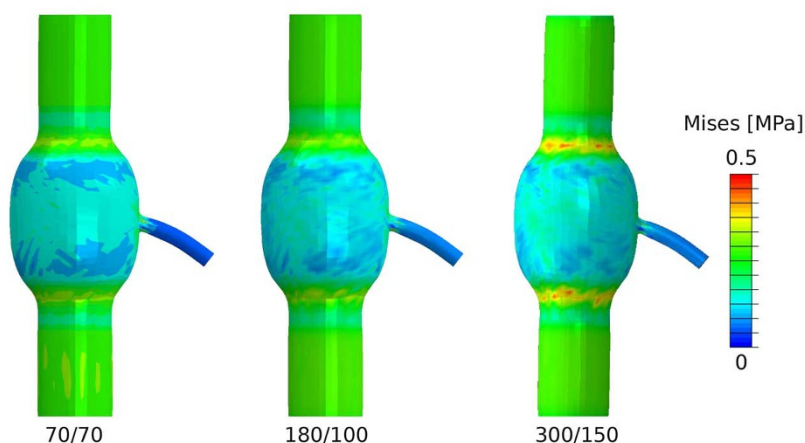


**Figure 6** | The maximal stress distribution pattern in the aortic wall after deployment of stents with strut thickness of 70/70, 180/100 and 300/150  $\mu\text{m}$ 's in the aortic wall, at 100 mmHg and 180 mmHg is depicted.

used as an adjunct therapy to endovascular repair if many segments are involved or it can be used as a palliative measure when surgery or endovascular repair is not feasible, in a patient with other associated severe co-morbidities seen in various clinical scenarios.

The study was performed in finite element analysis, and the results may vary in a patient model. However, finite element analysis method is a widely accepted method of evaluation, and previous simulation studies have correlated the usefulness of this method in various scenarios requiring virtual stent evaluation<sup>33</sup>. Further testing of the method needs to be performed in animal models.

The results of variations due to individual patient anatomy need to be studied further. We investigated an idealized geometry of the

aneurysm model. The effect of deployment of the device in a more complex patient based geometrical model with or without thrombus need to be studied. In individual cases with complex geometry, a patient based shape of the stent would be required. We presume complete apposition between the stent and aneurysmal wall, but in real life this is usually not the case as there is frequently some mural thrombus in the aneurysmal sac.

It should be emphasized that the presented simulations merely serve, as an indicative virtual proof-of-concept, and further in vitro and in vivo validation of the proposed concept seems highly advised. It should be stressed that the performed virtual tests may not be indicative of clinical performance without the previously mentioned necessary validation and verification.

**Table 2** | Changes in aortic diameter after deployment of stents of various strut thickness. The stent was covered by aortic tissue and covered by 1 mm thick tissue overgrowth

Maximum aneurysm diameter, (mm)	No stent	Stent 70/70 $\mu\text{m}$ , after embedding	Stent 180/100 $\mu\text{m}$ , after embedding	Stent 300/150 $\mu\text{m}$ , after embedding
AD <sub>0</sub> (0 mmHg)	59.4	59.3	59.6	60.7
AD <sub>100</sub> (100 mmHg)	65.8	62.7	62.6	63.2
AD <sub>180</sub> (180 mmHg)	68.4	64.5	64.1	64.4
AD <sub>180</sub> -AD <sub>100</sub>	2.6	1.8	1.5	1.2

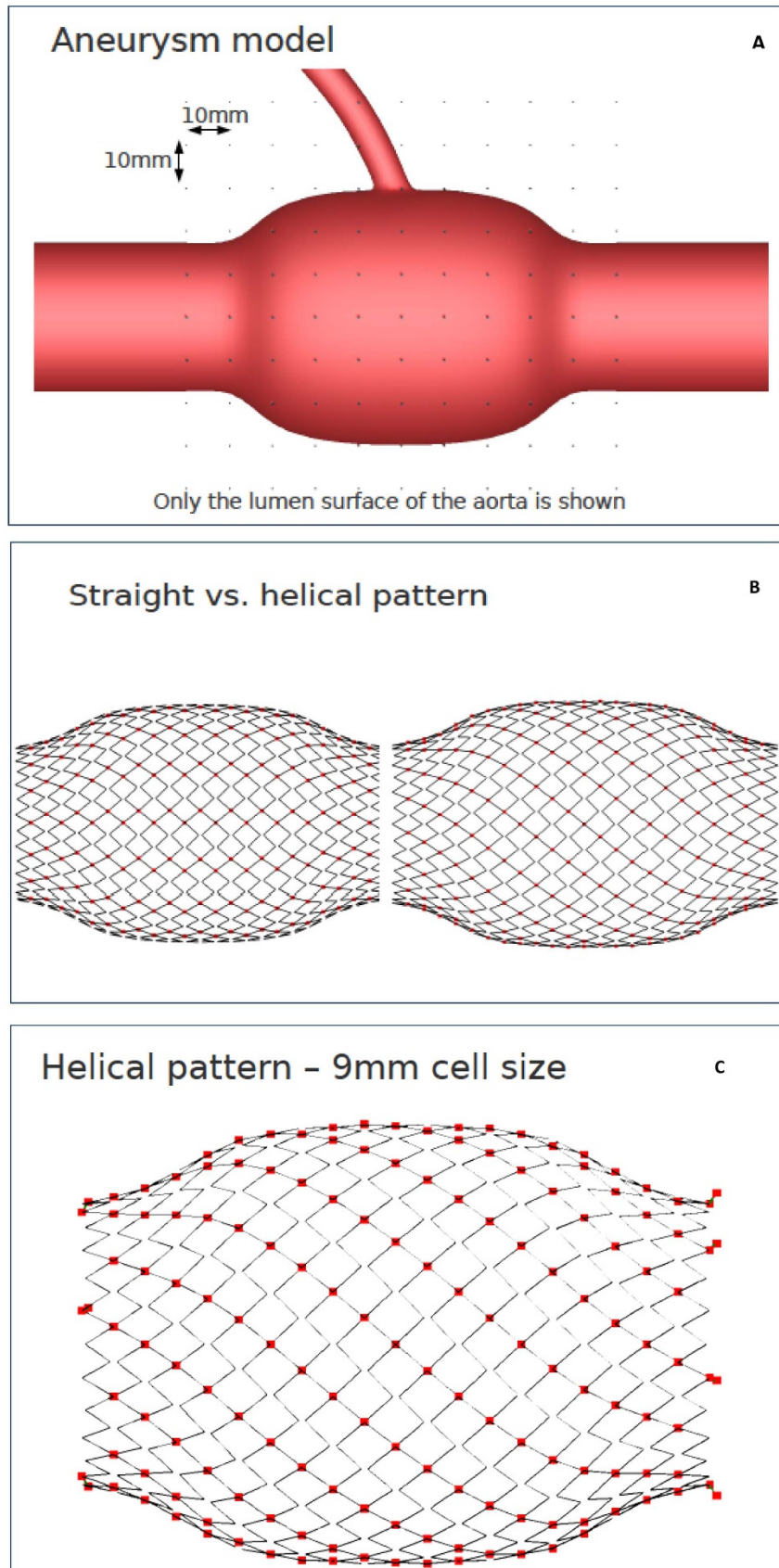


**Figure 7** | The aneurysm model used in the study is shown in Panel A. Panel B shows the helical and straight pattern of the stents developed in the study for testing. Panel C shows the enlarged view of the helical pattern of the stent used.

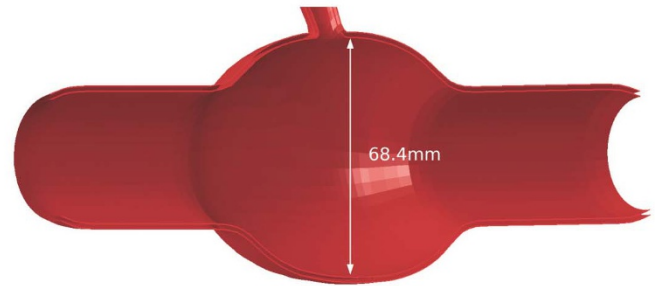




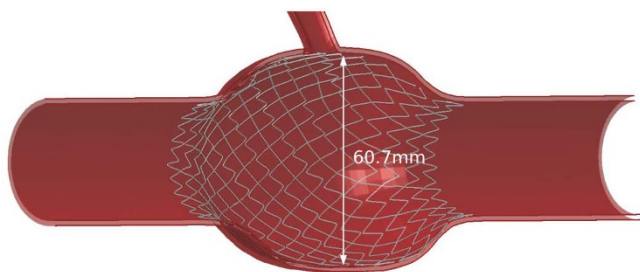
No stent @ 0mmHg



No stent @ 180mmHg

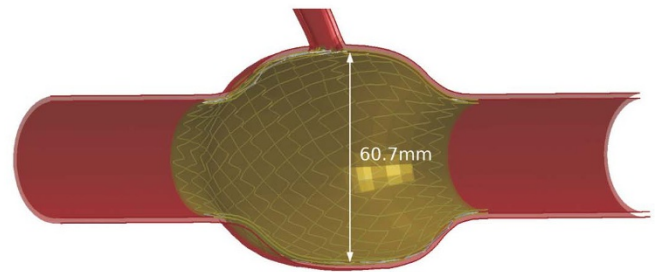


Stent embedded, 1mm tissue overgrowth @ 0mmHg



The tissue is not stress free:  
the stent chronic outward force increases the aneurysm diameter (AD) from 59.4 to 60.7mm

Stent embedded, 1mm tissue overgrowth @ 0mmHg



The 'old' tissue (red) is not stress free while the 'new' tissue (i.e. tissue added after overgrowth, in green) is stress free

Stent embedded, 1mm tissue overgrowth @ 180mmHg

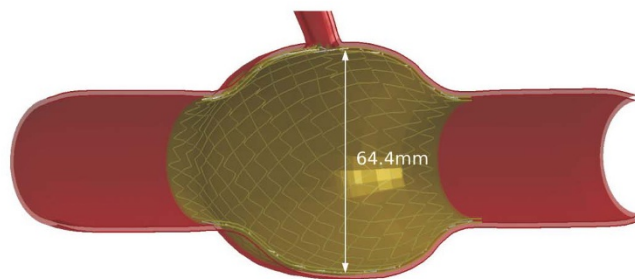


**Figure 8** | The aneurysm model before and after deployment of 300/150  $\mu\text{m}$  stent is shown. The stent was embedded and thereafter a model was created with a tissue overgrowth of 1 mm.

## Methods

**Strut selection for stage 1 and 2 analysis.** A self-expanding stent design model was developed initially with a stent strut thickness of 70  $\mu\text{m}$  and 70  $\mu\text{m}$  width. The study was done in 3 stages. In the first stage, the 70/70  $\mu\text{m}$  stent was chosen for study. The conventional existing peripheral stents have stent thickness of 200  $\mu\text{m}$ . Hence, for stage 1 evaluation, we chose a stent with thin struts of 70  $\mu\text{m}$  thickness and in the higher side for stage 2 analysis, a stent thickness of 300  $\mu\text{m}$  was chosen. In the beginning of the study we anticipated the stent to increase the aneurysm wall stresses due to its self-expanding nature, and hence a thin stent with a benchmark of 70/

70  $\mu\text{m}$  (thickness/width) was chosen for initial analysis. This is to demonstrate its efficacy, and the harmless nature of the stent on the aneurysm wall, and the adjacent normal aortic wall on either edges of aneurysm.

**Aneurysm model creation, stent design development and deployment characteristics.** Simultaneously, the deployment characteristics of the stent were studied. Figure 7 (upper panel) shows the aneurysm model, which is 6 cm in maximum diameter and 6 cm in length. We chose a 6 cm diameter virtual aneurysm model for the study, as a higher diameter aneurysm size i.e. 6.5 cm in the current



medical practice would be a recommendation for surgical correction. The stent was 10 mm more than the aneurysm model in width, and there was a 10 mm extension of the stent beyond the aneurysm on either end to the normal aorta, to study the properties of the stent on adjacent normal aorta after deployment (Figure 1). The aneurysm model and the disposition of the deployed stent are shown in the supplementary file. The deployed stent was in contact with aorta and aneurysm wall in systole and diastole. The stent was oversized to compensate for any foreshortening of the stent during deployment inside the aneurysm in all dimensions, and also for better apposition in the aortic and aneurysm's wall due to its self-expanding nature. In real life situation, mild foreshortening after deployment is expected due to inaccuracy in the calculation of aneurysm dimensions, the presence of clots, fluid structural interactions and insignificant buckling in the stent due to large stent with its self-expanding nature. Balloon angioplasty was not performed after deployment as this can weaken or damage the aneurysm and adjacent normal aortic wall.

The stent that was designed first had a 70/70  $\mu\text{m}$  square struts. After testing this basic stent model, parametric modifications of the stent thickness and cell width were done, and the study was performed. The stent and aneurysmal properties were studied after changing the cell widths parametrically. After parametric adjustments, we limited the stent for evaluation at 9 mm cell width and 300/150  $\mu\text{m}$ . This is due to its non-buckling nature, and higher radial force on the aneurysm wall with this 300/150  $\mu\text{m}$  compared to other stents with various strut thicknesses.

The daughter artery was modeled, and it is functionally equal to a major branch of the aorta, for example, a single renal artery. The daughter artery had a luminal diameter of 7 mm and wall thickness of 0.7 mm, and it had a luminal connection with the aneurysm. The origin of the daughter artery was 60 degrees from the aneurysm wall. Several stent designs were generated, both with straight or helical patterns, and with different cell sizes (Figure 7, Panel B). The stent was first crimped and then released in the aortic lumen.

**Finite element analysis.** For finite element modeling of aorta hyper-elastic matrix models of element type S4 (quadrilateral shells) was used<sup>34</sup>. Total number of elements in the aorta was 5040 (thickness of 1.5 mm) and the total elements in tissue overgrowth were 2171 (thickness of 1 mm). The nitinol material was a user subroutine of Abaqus<sup>35</sup>. For the nitinol material model the Abaqus subroutine for beam elements with 14 parameters was used. It models a possible Nitinol material at body temperature as described by Conti et al<sup>35</sup>. The total number of elements used were 4160 with element type of B31 (linear beams) with rectangular cross section. Modeling of embedding was performed using TIE constraints between tissue and the stent. The mesh sensitivity analysis was not performed. However, the mesh of stent was varied from 600 to 6000 elements and the mesh was chosen based on variation < 5% of peak radial force during radial force testing of 300/150  $\mu\text{m}$  stent with 9.5 cell unit (Figure 4). The mesh of the aneurysm's maximal diameter when inflated with a pressure of 180 mmHg changed by < 1% when doubling the number of elements.

The radial force testing was performed using a virtual rigid cylinder to decrease the stent diameter. The crimping was modeled using surface elements (FM3D4R). To simulate virtually the deployment of the novel stent into the aneurysm, the stress-free stent was first crimped using a crimping surface shaped as a cylinder with conical ends and then released inside the aorta. This release mechanism was simulated by activating the contact between the stent and aorta and thereby, increasing the radius of the crimping surface to a value above the aortic radius.

The stent was initially tested for buckling properties in cross sectional finite element analysis using Abaqus Explicit Solver, Simulia, 2012. The analysis was performed as quasi-static, ensuring that the kinetic energy was below 5% of the total energy. At cell width of 9 mm, there was no buckling of the stent.

#### Buckling properties, hemodynamic parameters and radial force measurements.

Buckling of stent during deployment would lead to inadequate apposition of the stent in aneurysm wall and reduce its ability to absorb wall stresses and remodeling of the wall. Hence, the 9 mm cell-width stent was chosen, and it was loaded on a mandrel and the stent was deployed inside the aneurysm. The stress-strain properties, contact pressures, the aortic and aneurysm shapes before and after stent implantation in the aneurysm were studied at 0, 100 and 180 mmHg. These pressures were chosen to maintain uniformity in observations and analysis of results in the study, and also for veracity. Blood pressure's upper limit was fixed at 180 mmHg, as in real life situation a blood pressure control to  $\leq$  180 mm Hg could be easily achieved by pharmacological measures. Except for stage 1 study, which was an initial proof-of-concept analysis to demonstrate the safety and feasibility of this new technique, in all other experiments, the upper limit of blood pressure for evaluation was fixed at 180 mmHg to maintain uniformity. In stage 1 study, the upper limit of blood pressure was fixed at 160 mmHg arbitrarily. The stent was of Nitinol material, and the aneurysm was an anisotropic hyper-elastic model. The aortic thickness was 1.5 mm and daughter artery's thickness was 0.7 mm. The stent strut dimensions (thickness/width) were increased to 180/100  $\mu\text{m}$  and 300/150  $\mu\text{m}$ . Thereafter, radial force testing on the aortic stent was done, and the results were tabulated. For radial force testing stent designs with 4 cell sizes were considered – 4.8, 4.9, 7.9 and 9.5 mm and three strut thickness/width were considered – 70/70, 180/100, 300/150  $\mu\text{m}$ .

**Stage 2 analyses with 300/150  $\mu\text{m}$  stent after embedding.** In stage 2 analyses, a prototype of 300/150  $\mu\text{m}$  (thickness/width) stent was tested in the aneurysm model for its effect on maximal wall stresses. This was chosen as it had a greater radial force compared to other stent's strut dimensions (70/70 and 180/100  $\mu\text{m}$ , figure 4), and hence it would have better stiffness and apposition in the aneurysm wall. As the

aneurysm wall occasionally has organized thrombus, a good radial force, essentially leads to better apposition of the stent.

Also, thicker or larger struts have a higher probability for tissue proliferation and better support to the aortic wall, and enhanced ability to absorb stresses. However, if the strut thickness is too high, it would lead to more damaging forces on the aortic wall due to the self-expanding nature of the stent. Hence the upper limit for evaluation was arbitrarily fixed at 300  $\mu\text{m}$  for the stage 2 study. The stent was embedded in the aortic wall initially, and later a model was created with a tissue overgrowth cover of 1 mm (Figure 8). This is an assumption that the stent may promote a tissue growth due to biophysical and chemical reaction, and a tissue cover would be formed over the entire stent after deployment.

**Stage 3 analyses with all the stents after embedding.** Subsequently, stage 3 analysis was performed using stents with struts (thickness/width) 70/70, 180/100 and 300/150  $\mu\text{m}$  in similar aortic aneurysm models after embedding the stent in aortic wall with a tissue cover of 1 mm. Comparison of the ability of the stents to reduce aortic wall stresses was studied. The larger stent struts could help to proliferate tissue overgrowth better which needs to be studied in tissue cultures.

- Guo, D. C., Papke, C. L., He, R. & Milewicz, D. M. Pathogenesis of thoracic and abdominal aortic aneurysms. *Ann N Y Acad Sci.* **1085**, 339–52 (2006).
- Karapanagiotidis, G. T. et al. Serum levels of matrix metalloproteinases 1, 2, 3 and 9 in thoracic aortic diseases and acute myocardial ischemia. *J Cardiothorac Surg.* **4**, 59 (2009).
- Danyi, P., Eleftheriades, J. A. & Jovin, I. S. Medical therapy of thoracic aortic aneurysms: are we there yet? *Circulation.* **124**, 1469–769 (2011).
- Vijay, S. R., Jae, K. O., Thoralf III, M. S. & Kim, A. E. Acute Aortic Syndromes and Thoracic Aortic Aneurysm. *Mayo Clin Proc.* **84**, 465–481 (2009).
- Lederle, F. A. et al. Outcomes following endovascular vs open repair of abdominal aortic aneurysm: A randomized trial. *JAMA.* **302**, 1535–1542 (2009).
- Schermerhorn, M. L. et al. Endovascular vs. open repair of abdominal aortic aneurysms in the Medicare population. *N Engl J Med.* **358**, 464–474 (2008).
- Geert, M., Marcel, K. & Sam, H. Complications after Endovascular Aneurysm Repair. *Semin Intervent Radiol.* **26**, 3–9 (2009).
- Shane, S. P. et al. Endoleaks after endovascular repair of thoracic aortic aneurysms. *J Vasc Surg.* **44**, 447–52 (2006).
- Greenhalgh, R., Brown, L., Kwong, G., Powell, J. & Thompson, S. Comparison of endovascular aneurysm repair with open repair in patients with abdominal aortic aneurysm (EVAR trial 1), 30-day operative mortality results: randomised controlled trial. *Lancet.* **364**, 818–20 (2004).
- Prinssen, M. et al. A randomized trial comparing conventional and endovascular repair of abdominal aortic aneurysms. *N Engl J Med.* **351**, 1677–18 (2004).
- Sultan, S. & Hynes, N. One-year results of the multilayer flow modulator stent in the management of thoracoabdominal aortic aneurysms and type B dissections. *J Endovasc Ther.* **20**, 366–77 (2013).
- Sfyroeras, G. S. et al. Flow-diverting stents for the treatment of arterial aneurysms. *J Vasc Surg.* **56**, 839–46 (2012).
- Melanie, B. S. et al. Perceptibility and Quantification of in-Stent Stenosis With Six Peripheral Arterial Stent Types in Vitro: Comparison of 16-MDCT Angiography, 64-MDCT Angiography, and MR Angiography. *American Journal of Roentgenology.* **194**, 1346–1351 (2010).
- Martin, S. et al. Inflammatory Response to Stent Implantation: Differences in Femoropopliteal, Iliac, and Carotid Arteries. *Radiology.* **224**, 529–535 (2002).
- Hall, A. J., Busse, E. F. G., McCarville, D. J. & Burgess, J. J. Aortic Wall tension as a predictive factor for abdominal aortic aneurysm rupture: improving the selection of patients for abdominal aortic aneurysm repair. *Ann Vasc Surg.* **14**, 152–157 (2000).
- Venkatasubramaniam, A. K. et al. A comparative study of the aortic wall stress using finite element analysis for ruptured and non-ruptured abdominal aortic aneurysms. *Eur J Vasc Endovasc Surg.* **28**, 168–176 (2004).
- Fillinger, M. F., Raghavan, M. L., Marra, S. P., Cronenwett, J. L. & Kennedy, F. E. In vivo analysis of mechanical wall stress and abdominal aortic aneurysm rupture risk. *J Vasc Surg.* **36**, 589–97 (2002).
- MacSweeney, S. T. Mechanical properties of abdominal aortic aneurysm and prediction of risk of rupture. *Cardiovasc Surg.* **1999**; **7**, 158–9 (1999).
- David, A. V. & Jonathan, P. V. G. Biomechanical Determinants of Abdominal Aortic Aneurysm Rupture. *ATVB.* **25**, 1558–1566 (2005).
- Topaz, O. & Vetrovec, G. W. The stentless stent: Mechanisms and revascularization options. *Cathet. Cardiovasc. Diagn.* **37**, 293–299 (1996).
- Kearney, M. et al. Histopathology of in-stent restenosis in patients with peripheral artery disease. *Circulation.* **95**, 1998–2002 (1997).
- Post, M. J., de Smet, B. J., van der Helm, Y., Borst, C. & Kuntz, R. E. Arterial remodeling after balloon angioplasty or stenting in an atherosclerotic experimental model. *Circulation.* **96**, 996–1003 (1997).
- Nugent, H. M. et al. Ultrasound-guided percutaneous delivery of tissue-engineered endothelial cells to the adventitia of stented arteries controls the response to vascular injury in a porcine model. *J Vasc Surg.* **56**, 1078–88 (2012).
- Bailey, B. M., Fei, R., Munoz-Pinto, D., Hahn, M. S. & Grunlan, M. A. PDMS star-PEG hydrogels prepared via solvent-induced phase separation (SIPS) and their potential utility as tissue engineering scaffolds. *Acta Biomaterialia.* **8**, 4324–33 (2012).



25. Bulick, A. *et al.* Impact of endothelial cells and mechanical conditioning on smooth muscle cell extracellular matrix production and differentiation. *Tissue Engineering*. **15**, 815–25 (2009).
26. Suncica, C., Ravi-Chandar, K., Zvonimir, K., Dragan, M. & Serguei, L. Mathematical model analysis of wallstent and aneuRx. Dynamic responses of bare-Metal endoprosthesis compared with those of Stent-Graft. *Tex Heart Inst J*. **32**, 555–55 (2005).
27. Rollo, P. V., Marcus, H. H. & Zvonimir, K. Regression of inflammatory abdominal aortic aneurysm after endoluminal treatment with bare-metal wallstent® endoprostheses. *Tex Heart Inst J*. **27**, 146–149 (2000).
28. Tang, X. *et al.* Clinical experience with multiple stents in complex thoraco-abdominal aortic aneurysms. *Chinese Medical Journal*. **126**, 3784–3786 (2013).
29. Li, Zhi-yong. Computed wall stress may predict the growth of abdominal aortic aneurysm. *Conf Proc IEEE Eng Med Biol Soc*. **2010**, 2626–9 (2010).
30. Shang, E. K. *et al.* Peak wall stress predicts expansion rate in descending thoracic aortic aneurysms. *Ann Thorac Surg*. **95**, 593–8 (2013).
31. Wilson, K. *et al.* The relationship between abdominal aortic aneurysm wall compliance, maximum diameter and growth rate. *Cardiovasc Surg*. **7**, 208–213 (1999).
32. Leung, J. H. *et al.* Relationship between growth rate and maximum wall stress in abdominal aortic aneurysms. *J Biomech*. **39**, S274 (2006).
33. Mortier, P., DeBeule, M., Segers, P., Verdonck, P. & Verhegghe, B. Virtual bench testing of the new generation coronary stents. *EuroIntervention*. **7**, 369–376 (2011).
34. Raghavan, M. L. & Vorp, D. A. Toward a biomechanical tool to evaluate rupture potential of abdominal aortic aneurysm: identification of a finite strain constitutive model and evaluation of its applicability. *J Biomech*. **33**, 475–482 (2000).
35. Conti, M. *et al.* Impact of carotid stent cell design on vessel scaffolding: a case study comparing experimental investigation and numerical simulations. *J. Endovasc. Ther.* **3**, 397–406 (2011).

## Acknowledgments

Sincere thanks to FEops, Ghent, Belgium for their excellent finite element analysis, and evaluation at every stage in the study.

## Author contributions

M.C.A. conceived the idea and method; design and modeling of the stent, prepared and edited the main manuscript text with figures; I.F.P. helped in manuscript preparation, comments and critical discussion in the study. Both authors reviewed the manuscript.

## Additional information

**Supplementary information** accompanies this paper at <http://www.nature.com/scientificreports>

**Competing financial interests:** The authors declare no competing financial interests.

**How to cite this article:** Arokiaraj, M.C. & Palacios, I.F. Finite Element Modeling of A Novel Self-Expanding Endovascular Stent Method in Treatment of Aortic Aneurysms. *Sci. Rep.* **4**, 3630; DOI:10.1038/srep03630 (2014).



This work is licensed under a Creative Commons Attribution-NonCommercial-NoDerivs 3.0 Unported license. To view a copy of this license, visit <http://creativecommons.org/licenses/by-nc-nd/3.0>

# SCIENTIFIC REPORTS

**OPEN**

## Corrigendum: Finite Element Modeling of A Novel Self-Expanding Endovascular Stent Method in Treatment of Aortic Aneurysms

Mark C. Arokiaraj, Gianluca De Santis, Matthieu De Beule & Igor F. Palacios

*Scientific Reports* 4:3630; doi: 10.1038/srep03630; published online 10 January 2014; updated on 20 February 2017

Gianluca De Santis and Matthieu De Beule were omitted from the author list in the original version of this Article. This has now been corrected in the HTML version of the Article.

The Author Contributions section now reads:

M.C.A. conceived the idea and method; design and modelling of the stent and aneurysm, prepared and edited the main manuscript text with figures; G.D.S. and M.D.B. performed the finite element simulations and contributed to the finite element study details in the methodology section; I.F.P. supervised the work, helped in manuscript preparation, comments and critical discussion in the study. All authors reviewed the manuscript.



This work is licensed under a Creative Commons Attribution-NonCommercial-NoDerivs 3.0 Unported License. To view a copy of this license, visit <http://creativecommons.org/licenses/by-nc-nd/3.0/>

© The Author(s) 2017